ChemComm

COMMUNICATION

(3E,7E)-3,7-Bis(2-oxoindolin-3-ylidene)-5,7-dihydropyrrolo[2,3-f]indole-2,6(1H,3H)-dione based polymers for ambipolar organic thin film transistors†

Yinghui He, Chang Guo, Bin Sun, Jesse Quinn and Yuning Li*

A novel acceptor, (3E,7E)-3,7-bis(2-oxoindolin-3-ylidene)-5,7-dihydro-pyrrolo[2,3-f]indole-2,6(1H,3H)-dione, was reported. Donor–acceptor (D–A) polymer semiconductors using this new building block showed high ambipolar charge transport performance with hole and electron mobilities up to 0.19 and 0.09 cm² V⁻¹ s⁻¹, respectively, in thin film transistors.

Polymer semiconductors are useful materials for low-cost organic electronics such as organic thin film transistors (OTFTs)[1,2] and organic photovoltaics (OPVs)[3,4] due mainly to their excellent solution processability and mechanical robustness. In recent years, a number of donor–acceptor (D–A) π-conjugated polymers have demonstrated high mobility in OTFTs.[5–7] In these high-performance D–A polymers, the intermolecular D–A interaction of the donor and acceptor building blocks could shorten the π–π stacking distance and thus improve the interchain charge transport. Intensified research effort has been devoted to the development of novel electron donor and acceptor building blocks in order to enhance the charge carrier mobility for a wider range of applications of polymer semiconductors.[8,9] Recently our group reported a novel acceptor building block, (3E,7E)-3,7-bis(2-oxoindolin-3-ylidene)benzo[1,2-b:4,5-b']difuran-2,6(3H,7H)-dione (IBDF, Fig. 1a),[10] which has been used for D–A polymers for OTFTs.[10–15] Owing to the strong electron withdrawing capability of IBDF, IBDF-based D–A polymers showed excellent n-type and ambipolar charge transport performance with a high electron mobility up to 1.74 cm² V⁻¹ s⁻¹.[12]

In this study, we designed and synthesized a novel acceptor building block, namely (3E,7E)-3,7-bis(2-oxoindolin-3-ylidene)-5,7-dihydropyrrolo[2,3-f]indole-2,6(1H,3H)-dione (IBDP, Fig. 1a), which is a structural analogue to IBDF, where the lactones in the

Department of Chemical Engineering and Waterloo Institute for Nanotechnology (WIN), 200 University Ave W, Waterloo, Ontario, N2L 3G1, Canada.
E-mail: yuning.li@uwaterloo.ca; Fax: +1-519-888-4347;
Tel: +1-519-888-4567 ext. 31105
† Electronic supplementary information (ESI) available: Detailed procedures for the synthesis and device fabrication, and additional data. See DOI: 10.1039/c5cc01021g
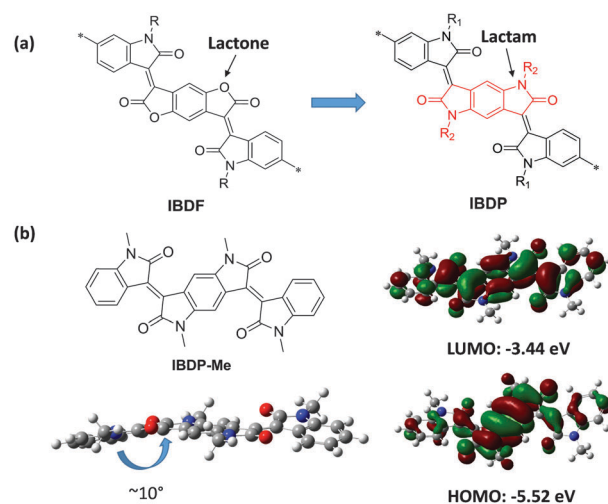

Fig. 1 (a) Structure of IBDF and IBDP; (b) structure of IBDP–Me, its optimized geometry, LUMO and HOMO distribution through computational calculation.

IBDF core are replaced with lactams in the IBDP core. Previously it was found that the IBDF-based polymers required giant substituents such as 4-octadecyldocosyl (containing 40 carbon atoms) to render polymers soluble in commonly used solvents such as chloroform.[10,12] Unfortunately, precursors to such large substituents are not readily available. This makes the optimization of IBDF-based polymers difficult. The newly designed IBDP core allows for substitution at four nitrogen atoms, potentially enabling solubilisation of the IBDP-based polymers with more easily accessible shorter substituents. We synthesized an IBDP compound (7 in Scheme 1) with readily available dodecyl and 2-decyltetradecyl substituents and used this IBDP unit as an acceptor and bithiophene or (E)-1,2-di(thiophen-2-yl)ethane as a donor to form two D–A polymers (P1 and P2). Both polymers showed high ambipolar charge transport performance.
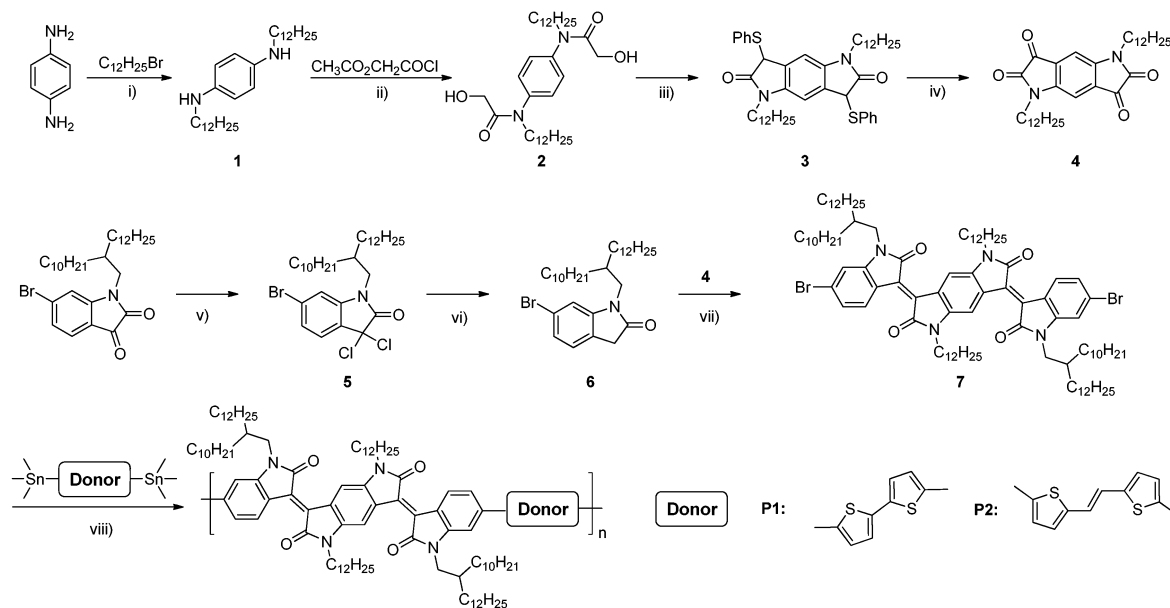
We started our study by conducting computational simulations on two model compounds: IBDF–Me (see ESI†) and IBDP–Me (Fig. 1b). The simulation results showed that IBDP–Me has a very small dihedral angle (∼10°) between an indolin-2-one

Scheme 1 Synthetic route to the IBDP monomer and polymers: (i) ethanol/reflux; (ii) $CH_2Cl_2/Et_3N/0$ °C to r.t.; THF/MeOH/H_2O/K_2CO_3/r.t.; (iii) CH_2Cl_2/ oxalyl chloride/DMSO/$Et_3N/-78$ °C to r.t.; CH_2Cl_2/thiophenol/TFAA/$BF_3·Et_2O$/r.t.; (iv) THF/H_2O/ammonium cerium nitrate/r.t.; (v) toluene/PCl_5/r.t.; (vi) AcOH/Zn/r.t.; (vii) AcOH/HCl/reflux; (viii) chlorobenzene/P(o-tolyl)$_3$/Pd_2(dba)$_3$/120 °C.

unit and the 5,7-dihydropyrrolo[2,3-f]indole-2,6-(1H,3H)-dione core, which is comparable to that of IBDF–Me ($\sim 8°$). As for the frontier orbitals, the highest occupied molecular orbital (HOMO)/ the lowest unoccupied molecular orbital (LUMO) energy levels were predicted to be -6.11 eV/-3.78 eV and -5.52 eV/-3.44 eV for IBDF–Me and IBDP–Me, respectively, suggesting that IBDP is a weaker acceptor than IBDF.

The syntheses of the IBDP monomer (**7**) and polymers (**P1** and **P2**) are outlined in Scheme 1. First, p-phenylenediamine was N,N'-dialkylated with dodecyl bromide in ethanol to form **1**, which was used to prepare **4** following a similar synthetic route reported previously.[16] Compound **6** was synthesized using a modified literature method.[17] Specifically, 6-bromo-1-(2-decyltetradecyl)indoline-2,3-dione was first chlorinated with PCl_5 to give intermediate **5**, which was reduced with zinc to form **6**. Condensation of **4** with two equivalents of **6** in refluxing acetic acid in the presence of a catalytic amount of HCl afforded monomer **7**. Two IBDP-based polymers **P1** and **P2** were synthesized *via* the Stille coupling polymerization of **6** with 5,5′-bis(trimethyl-stannyl)-2,2′-bithiophene and (*E*)-1,2-bis(5-(trimethylstannyl)thio-phen-2-yl)ethene, respectively. The crude polymers were purified by Soxhlet extraction successively using acetone and hexanes to remove the oligomers and other impurities. Finally the polymers were dissolved in chloroform to afford **P1** and **P2** in yields of 82% and 98%, respectively. Both polymers have very good solubility in several common solvents such as chloroform, toluene, chlorobenzene, and 1,2-dichlorobenzene at room temperature. The molecular weights of these polymers were measured by gel-permeation chromatography (GPC) at 80 °C with chlorobenzene as an eluent and polystyrene as standard. The number average molecular weight (M_n) and the polydispersity index (PDI) were determined to be 128 kDa and 2.89 for **P1** and 158 kDa and 1.59 for **P2**. The thermal stability of the

polymers was characterized by thermogravimetric analysis (TGA). A 5% weight loss was observed at 384 °C for **P1** and 380 °C for **P2**, indicating good thermal stability of both polymers (ESI†).

The UV-Vis-IR absorption spectra of the polymers in solution and in thin films are shown in Fig. 2. Both polymers exhibited typical dual band absorption, wherein the low energy band can be attributed to the internal charge transfer (ICT) transition and the high energy band originates from the $\pi-\pi^*$ transition.[18,19] In solution, the maximum absorption wavelengths (λ_{max}) are 699 nm for **P1** and 711 nm for **P2**. The λ_{max} of the **P1** film remained at 699 nm, but a prominent shoulder at 822 nm appeared, indicating the more extended conjugation of the polymer chains in the solid state. Interestingly, **P2** showed a blue-shift in absorption from solution (711 nm) to the film
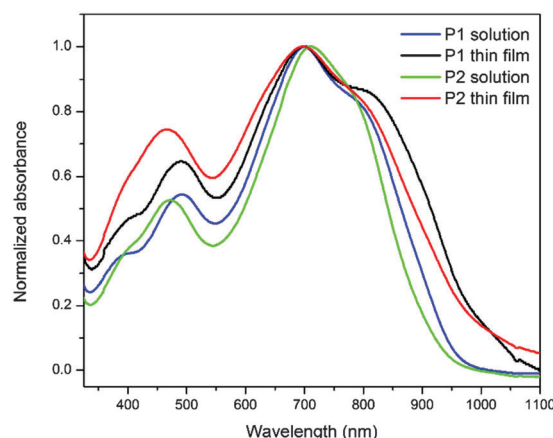

Fig. 2 The UV-Vis-IR absorption spectra in solution (chloroform) and in thin films.

(698 nm), which might be induced by the H-aggregation-type interchain packing in the solid state.[20,21] The optical band gaps of the polymer films are calculated to be 1.23 eV for **P1** and 1.22 eV for **P2** using the absorption onsets. Cyclic voltammetry (CV) was used to reveal electrochemical properties of the polymers (ESI†). By using the oxidation onset potentials, HOMO levels were calculated to be -5.60 eV and -5.71 eV for **P1** and **P2**, respectively. LUMO levels were calculated from the reduction onset potentials to be -3.71 eV and -3.70 eV for **P1** and **P2**, respectively. The band gaps obtained from the CV (**P1**: 1.89 eV; **P2**: 2.01 eV) are larger than their optical band gaps, which might be due to the large exciton binding energy that can be as high as ~ 0.4–1.0 eV.[22,23]

P1 and **P2** were evaluated as channel semiconductors in bottom-gate, bottom-contact OTFT devices fabricated on dodecyl-trichlorosilane (DDTS) modified SiO_2/Si wafer substrates. Both polymers showed ambipolar charge transport behaviour (see detailed device data in the ESI†). For devices based on **P1**, the best performance with a hole mobility of 0.19 $cm^2\ V^{-1}\ s^{-1}$ and an electron mobility of 0.088 $cm^2\ V^{-1}\ s^{-1}$ was achieved for the 150 °C-annealed films (Fig. 3). Annealing at a higher temperature of 200 °C led to a slight increase in the electron mobility (up to 0.089 $cm^2\ V^{-1}\ s^{-1}$), but a significant drop in the hole mobility (0.057 $cm^2\ V^{-1}\ s^{-1}$). For devices based on **P2**, the best overall performance with hole/electron mobilities of 0.10 $cm^2\ V^{-1}\ s^{-1}$/0.075 $cm^2\ V^{-1}\ s^{-1}$ was obtained for the 200 °C-annealed polymer films (ESI†). Annealing at a higher temperature of 250 °C did not further improve the device performance. We noticed that **P1** and **P2** showed lower charge transport performance than some of the IBDF based polymers.[12,15] One possible reason for their lower mobility is that an optimal side

chain combination is not reached in these polymers. **P1** and **P2** showed greatly improved solubility due to the presence of four large side chains on IBDP. However, the excessively strong side chain interaction in the solid state might hinder the π–π stacking of the polymer main chains. The very weak diffraction peaks corresponding to the π–π stacking distances for both polymers might substantiate this side chain interference (see the ESI† data and later discussions). Using shorter side chains may help strengthen the π–π interaction. Furthermore, most of the high mobility IBDF polymers reported so far bear the 4-octadecyldocosyl side chain, which is at a farther distance from the polymer backbone compared to the 2-decyltetradecyl side chain in **P1** and **P2**. The branching point of branched side chains was reported to have a great impact on the ordering of the polymer chains and the carrier mobility.[11,20,24] The use of branched side chains with a larger spacer between the branching point and the backbone such as 4-decylhexadecyl or four straight alkyl side chains on IBDP may lead to better charge transport performance.

Transmission X-ray diffraction (XRD) measurement was performed on polymer flakes of both polymers. **P1** and **P2** showed intense primary diffraction peaks at 2θ = 3.26° and 3.51°, which correspond to the interlayer lamellar d-spacing of 2.71 nm and 2.52 nm, respectively. The weak diffraction peak at 2θ = 25.04° for P1 originates from the π–π stacking distance of polymer chains, which was calculated to be 0.355 nm. No noticeable π–π stacking peak was observed for **P2**, which might explain the lower performance observed for **P2** than for **P1**. The presence of four long side chains on IBDP might hinder the π–π stacking and lead to the lower carrier mobility of these IBDP polymers compared to the IBDF polymers as discussed previously. The surface morphology of **P1** and **P2** thin films spin-coated on DDTS modified SiO_2/Si wafer substrates was examined by atomic force microscopy (AFM). **P1** thin films showed fibre-like domains, which grew slightly as the annealing temperature increased from 100 °C to 150 °C and remained similar at an annealing temperature of 200 °C. In general, **P2** thin films showed poorly defined domains compared to **P1** films, indicative of the less ordered chain packing of **P2**.

In conclusion, a novel electron-accepting building block, IBDP, is designed, synthesized, and incorporated into D–A polymers. Two IBDP-based polymers showed good solution processability and exhibited a high ambipolar semiconductor performance in OTFTs with a hole mobility up to 0.19 $cm^2\ V^{-1}\ s^{-1}$ and an electron mobility up to 0.09 $cm^2\ V^{-1}\ s^{-1}$. Our preliminary results demonstrated that IBDP is a promising electron acceptor building block for polymer semiconductors.

Fig. 3 Output (top) and transfer (bottom) curves of an OTFT device based on a thin film of **P1** annealed at 150 °C.

Notes and references

1 C. Guo, W. Hong, H. Aziz and Y. Li, *Rev. Adv. Sci. Eng.*, 2012, **1**, 200–224.
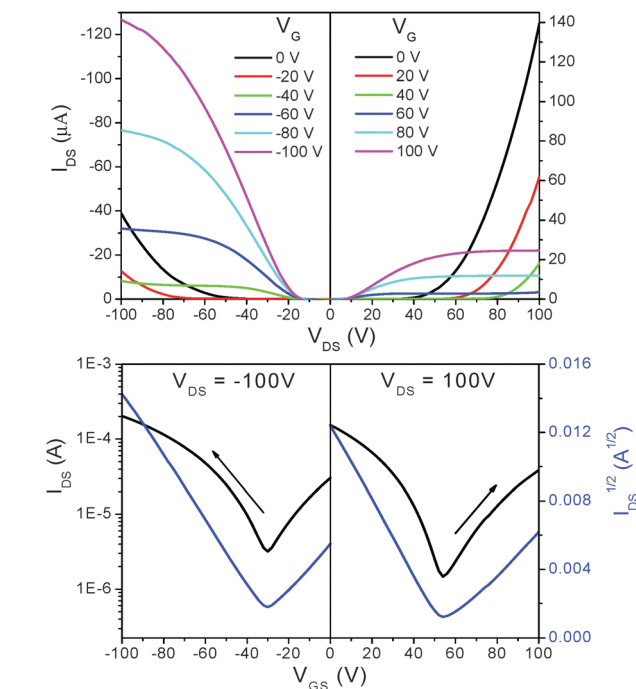2 Y. Li, P. Sonar, L. Murphy and W. Hong, *Energy Environ. Sci.*, 2013, **6**, 1684–1710.

3 P. L. T. Boudreault, A. Najari and M. Leclerc, *Chem. Mater.*, 2011, **23**, 456–469.

4 G. Li, R. Zhu and Y. Yang, *Nat. Photonics*, 2012, **6**, 153–161.

5 X. Guo, M. Baumgarten and K. Müllen, *Prog. Polym. Sci.*, 2013, **38**, 1832–1908.

6 J. D. Yuen and F. Wudl, *Energy Environ. Sci.*, 2013, **6**, 392–406.

7 G. Kim, S.-J. Kang, G. K. Dutta, Y.-K. Han, T. J. Shin, Y.-Y. Noh and C. Yang, *J. Am. Chem. Soc.*, 2014, **136**, 9477–9483.

8 Y. He, W. Hong and Y. Li, *J. Mater. Chem. C*, 2014, **2**, 8651–8661.

9 K.-J. Baeg, M. Caironi and Y.-Y. Noh, *Adv. Mater.*, 2013, **25**, 4210–4244.

10 Z. Yan, B. Sun and Y. Li, *Chem. Commun.*, 2013, **49**, 3790–3792.

11 J.-H. Dou, Y.-Q. Zheng, T. Lei, S.-D. Zhang, Z. Wang, W.-B. Zhang, J.-Y. Wang and J. Pei, *Adv. Funct. Mater.*, 2014, **24**, 6270–6278.

12 T. Lei, J.-H. Dou, X.-Y. Cao, J.-Y. Wang and J. Pei, *Adv. Mater.*, 2013, **25**, 6589–6593.

13 T. Lei, J.-H. Dou, X.-Y. Cao, J.-Y. Wang and J. Pei, *J. Am. Chem. Soc.*, 2013, **135**, 12168–12171.

14 T. Lei, X. Xia, J.-Y. Wang, C.-J. Liu and J. Pei, *J. Am. Chem. Soc.*, 2014, **136**, 2135–2141.

15 G. Zhang, P. Li, L. Tang, J. Ma, X. Wang, H. Lu, B. Kang, K. Cho and L. Qiu, *Chem. Commun.*, 2014, **50**, 3180–3183.

16 J. W. Rumer, M. Levick, S.-Y. Dai, S. Rossbauer, Z. Huang, L. Biniek, T. D. Anthopoulos, J. R. Durrant, D. J. Procter and I. McCulloch, *Chem. Commun.*, 2013, **49**, 1–3.

17 A. N. C. Lötter, R. Pathak, T. S. Sello, M. a. Fernandes, W. A. L. van Otterlo and C. B. de Koning, *Tetrahedron*, 2007, **63**, 2263–2274.

18 P. M. Beaujuge, C. M. Amb and J. R. Reynolds, *Acc. Chem. Res.*, 2010, **43**, 1396–1407.

19 J. Kim, A.-R. Han, J. Hong, G. Kim, J. Lee, T. J. Shin, J. H. Oh and C. Yang, *Chem. Mater.*, 2014, **26**, 4933–4942.

20 T. Lei, J.-H. Dou and J. Pei, *Adv. Mater.*, 2012, **24**, 6457–6461.

21 J. Shin, H. A. Um, D. H. Lee, T. W. Lee, M. J. Cho and D. H. Choi, *Polym. Chem.*, 2013, **4**, 5688.

22 N. S. Sariciftci, *Primary photoexcitations in conjugated polymers: molecular exciton versus semiconductor band model*, World Scientific, 1997, ch. 4.

23 Y. Zhu, R. D. Champion and S. A. Jenekhe, *Macromolecules*, 2006, **39**, 8712–8719.

24 S. Chen, B. Sun, W. Hong, H. Aziz, Y. Meng and Y. Li, *J. Mater. Chem. C*, 2014, **2**, 2183.